Dynamic response of the thermometric net radiometer

J.D. Wilson [a,*], W.J. Massman [b], G.E. Swaters [c]

[a] Department of Earth & Atmospheric Sciences, University of Alberta, 1-26 Earth Sciences Building, Edmonton, Alberta, Canada T6G 2E3
[b] U.S. Forest Service, Fort Collins, CO, USA
[c] Department of Mathematics and Statistics, University of Alberta, Edmonton, Alberta, Canada

ARTICLE INFO

ABSTRACT

We computed the dynamic response of an idealized thermometric net radiometer, when driven by an oscillating net longwave radiation intended roughly to simulate rapid fluctuations of the radiative environment such as might be expected during field use of such devices. The study was motivated by curiosity as to whether non-linearity of the surface boundary conditions implies the existence of a non-vanishing mean signal even when mean forcing (i.e. mean net radiation) vanishes. These simulations do not prove (and owing to discretization and roundoff error, cannot prove) such a bias is absolutely non-existent, however they establish that the bias is of negligible practical importance, even for unrealistically large fluctuations in the net radiation. Other aspects of net radiometer design must account for the serious errors known to sometimes result (in the case of many devices), from field application of steady-state calibration factors.

© 2009 Elsevier B.V. All rights reserved.

1. Introduction

Several authors have considered the possibility that the net radiation measurement may be the seat of the widely reported energy balance closure problem, often presupposing that time variation of the radiative fluxes *on turbulence timescales* need not be considered. However by virtue of the boundary conditions on its upper and lower planes, the equations governing the response of a thermometric radiometer are non-linear, raising the possibility that, if either or both of the upward and downward longwave flux densities $(L_\uparrow, L_\downarrow)$ do vary in time on frequencies f that are rapid compared to the reciprocal of the thermal time constant of the device (roughly, $d^2/\kappa \sim 10$ s; κ is the thermal diffusivity and d is the thickness of the substrate), a mean signal may be produced even in the absence of a mean net longwave flux density $\overline{L^*} = \overline{L}_\uparrow - \overline{L}_\downarrow$. Since the longwave fluxes certainly do fluctuate on rapid timescales, in response to the spectrum of air temperature fluctuations, the passage of clouds, and possible variation of plant canopy and ground temperatures, such a bias (if significant in magnitude) would compromise use of this type of instrument, or at least demand a correction. Laboratory and field studies of a range of net radiometers led Smith et al. (1997) to conclude there is "a fundamental deficiency in the two-sided thermopile design used in most net pyrradiometers under non-equilibrium conditions."

Where measurements fail to close the energy balance, it is generally found that the sum $Q_H + Q_E$ of the convective fluxes (of sensible and latent heat, respectively) underestimates the available energy $Q^* - Q_G - \Delta Q_S$ (where Q^* is the net radiation, Q_G is the soil heat flux density, and ΔQ_S any storage term). Accordingly, many authors have considered that the seat of the problem lies with estimation of the convective fluxes[1]. However Kohsiek et al. (2007) focused on the radiative fluxes (as measured by thermometric radiometers), and indicate a possibility that the radiation term may lie at the root of the problem (though these authors assumed that error in Q^*, if present, would have arisen from spatial inhomogeneity of the site, or from radiometer calibration inaccuracy; they did not question the *principle* of the thermometric radiometer). Mauder et al. (2007), participants in the same experiment (EBEX-2000), recommend that "net radiation is preferably to be inferred from its four components, rather than measured directly." Echoing Brotzge and Duchon (2000) they note that "no international agreement exists on a radiation standard and calibration procedure" for the pyrgeometer (i.e. hemispheric longwave radiometer) and that "there is no agreement on the mathematical description of the physics of the instrument." As regards the latter, according to Mauder et al. the World Radiation

---

* Corresponding author. Tel.: +1 780 492 0353.
E-mail address: jaydee.uu@ualberta.ca (J.D. Wilson).

[1] On the basis of Large Eddy Simulations Huang et al. (2008) reported, as have earlier authors, that the underlying cause of the energy balance closure problem is (or can be) inadequate spatial representativity of point measurements of the vertical fluxes.

Center recommends the formula given by Philipona et al. (1995, Eq. (11)) and which was earlier derived by Albrecht et al. (1974, Eq. (9)), viz.:

$$L^* = \frac{U_{emf}}{C}(1 + k_1 \sigma T_B^3) + k_2 \sigma T_B^4 - k_3 \sigma (T_D^4 - T_B^4), \qquad (1)$$

where U_{emf} is the thermopile voltage, T_B the temperature of the cold junction of the thermopile, T_D the dome temperature, and C, k_1, k_2, k_3 are the calibration constants. Eq. (1) takes account of the differing temperatures of the dome and the substrate; it was derived assuming a steady radiation environment and steady temperature distribution within the device and, for that reason, will be of no further interest to us here.

2. Analysis of an idealized net radiometer

We wish to establish whether the *mean* temperature gradient induced in a thermometric net radiometer is a function (uniquely) of the *mean* net radiative flux density, irrespective of the steadiness (or otherwise) of the radiation field, and irrespective of any constraint on the magnitude of fluctuations in the radiometer's substrate temperature. We idealize the device as a slab (Fig. 1) whose material properties and whose temperature are uniform on the horizontal axes (one-dimensional treatment): the 'signal' is the difference $\Delta T = T_u - T_b$ in temperature between the upper and lower surfaces. We ignore shortwave radiation entirely, and adopt the two-stream approach to describe the longwave radiation field. We assume the upper and lower surfaces have the same emissivity ϵ, which is also the absorptivity. We neglect any convective heat fluxes, and ignore the realities of radiative interaction with the dome that would need to be used to effect that simplification. Furthermore we treat the material properties as independent of temperature, so that from the mathematical point of view we have a linear equation (the 'heat equation') subject to non-linear boundary conditions.

2.1. Dimensional analysis

The properties of primary relevance to the temporal response of the radiometer substrate are its conductivity (k, W m^{-1}K^{-1}); specific heat capacity (c_s, J kg^{-1}K^{-1}); density (ρ_s, kg m^{-3}); and thickness (d). The thermal diffusivity ($\kappa = k\rho_s^{-1}c_s^{-1}$, m^2 s^{-1}) is not an independent quantity. These properties entail four ($m = 4$) fundamental dimensions, e.g. length, time, mass, temperature. Now if we focus on the time constant τ, we have five ($n = 5$) variables of interest, and can expect an explicit prediction since

Fig. 1. Definitional schematic of idealized thermometric radiometer, and associated mathematical model.

$n - m = 1$. By inspection:

$$\frac{\tau}{d^2\kappa^{-1}} = \alpha, \qquad (2)$$

where Funk (1960) cites a result by Ingersoll that indicates $\alpha \sim 0.5$ (note: where τ is cited later, we have evaluated Eq. (2) with $\alpha = 1/2$, however the correctness of our results does not hinge on this choice). For an order of magnitude estimate of τ, we may take the radiometer described by Fritschen (1965): here an epoxy substrate ($\kappa \sim 10^{-7}$ m^2 s^{-1}) had a depth $d \sim 0.003$ m, and Fritschen measured the time constant to be 12 s (while Eq. (2) gives about 45 s). Halldin and Lindroth (1992; their Table 1) and Smith et al. (1997; their Tables 1a, b) confirm that most modern net radiometers have a time constant in the range 20–40 s, although faster devices do exist (e.g. Brotzge and Duchon, 2000; Cobos and Baker, 2003).

2.2. Governing equations

Conservation of energy on the upper and lower planes requires:

$$0 = \epsilon L_\downarrow(t) - \epsilon \sigma T_u^4(t) - k\left(\frac{\partial T}{\partial z}\right)_u, \qquad (3)$$

$$0 = \epsilon L_\uparrow(t) - \epsilon \sigma T_b^4(t) + k\left(\frac{\partial T}{\partial z}\right)_b, \qquad (4)$$

and these equations furnish the boundary conditions for the heat budget within the substrate,

$$c_s\rho_s\frac{\partial T}{\partial t} = -\frac{\partial}{\partial z}\left(-k\frac{\partial T}{\partial z}\right) = k\frac{\partial^2 T}{\partial z^2} \qquad (5)$$

(for convenience, we will define $c = \rho_s c_s$, the volumetric heat capacity). An initial condition:

$$T(z, 0) = f_0(z) \qquad (6)$$

completes the mathematical specification, where we shall set $f_0(z) = T_0 = $ const., the 'background' temperature.

Due to the non-linearity of the boundary conditions we have a non-linear system, and we believe that a general and exact solution for the response to time-dependent forcing, even if limited to the case of sinusoidal forcing (e.g. in one or both of $L_\downarrow, L_\uparrow$), cannot be obtained. The difficulty can be seen if one envisages a spectral decomposition of the temperature profile within the device, for the non-linear boundary conditions guarantee wave–wave interaction, that is, irrespective of the state at time t, (spectral) energy must propagate from the modes present at time t to an expanding range of harmonics. Suppose, for example, that the decomposition for T_u entailed a 'kth' (arbitrary) mode, viz. $a_k(t)\sin(2\pi kz/d)$. The upper boundary condition would involve $\sin^4(2\pi kz/d) \equiv [3 - 4\cos(4\pi kz/d) + \cos(8\pi kz/d)]/8$, and as a consequence there would be contributions to the amplitude-tendencies ($\partial a_{2k}/\partial t, \partial a_{4k}/\partial t$) of the ($2k, 4k$) harmonics. Conductive smoothing, proportional to k^2, will of course moderate this spectral transfer towards the higher wavenumbers.

Thus one cannot hope to find an exact and general dynamic solution. The textbook treatment of the radiometer (given later in Section 2.5) is limited to the steady-state case, and yields an analytical relationship linking $\Delta T(t) \equiv T_u(t) - T_b(t)$ which is sensed by a thermopile, to the net radiation $L^*(t) \equiv L_\downarrow(t) - L_\uparrow(t)$.

2.3. Implications of the non-linear boundary condition

We are interested in the undoubted time variation of the radiation fluxes ($L_\downarrow, L_\uparrow$) incident on a radiometer in the field, and more specifically whether their variability might cause a radio-

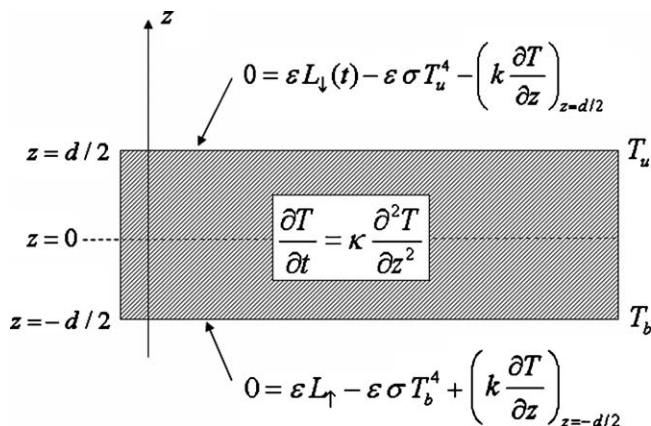meter bias (in the sense that the mean signal $\overline{\Delta T}$ did not vanish even when the mean net radiation $\overline{L^*}$ did). It is helpful to envisage an equilibrium (or reference) state, in which the radiometer itself and its environment (near and remote) are in an isothermal equilibrium at temperature T_0: the incident radiation fluxes are $L_\downarrow = L_\uparrow = \sigma T_0^4$, of which a fraction ϵ is absorbed by the device (which itself radiates at rate $\epsilon \sigma T_0^4$). The environmental net radiation is zero, the net rate of radiative energy supply to the device itself is zero, and there is no output signal ($T_u - T_b = 0$).

But now suppose we add an offset $A(t)$ to the downward radiative flux (for argument's sake) such that $L_\downarrow = L_\uparrow + A(t) = \sigma T_0^4 + A(t)$. Then:

(i) If $A(t)$ is sinusoidal one may assume there will be (at asymptotically large time after initialization) a sinusoidal component to the temperature T_u of the upper plane, such that $T_u(t) = \overline{T}_u + A_u \sin(2\pi f t)$, where the overbar denotes the mean over exactly one forcing cycle. A simple integration proves that

$$\overline{T_u^4} - \overline{T}_u^4 \equiv \frac{3}{8}A_u^4 + 3\overline{T}_u^2 A_u^2, \tag{7}$$

and so the resulting mean rate of emission of longwave radiative energy from the upper plane will exceed $\epsilon \sigma \overline{T}_u^4$.

(ii) Without restriction on the form of $T_u(t)$, if we write $T_u(t) = \overline{T}_u + T'_u$ (where the overbar no longer carries the implication of being an average over one forcing cycle) then it follows that

$$\overline{T_u^4} - \overline{T}_u^4 = \overline{T'^4_u} + 6\overline{T}_u^2\,\overline{T'^2_u} + 4\overline{T}_u\overline{T'^3_u}. \tag{8}$$

This again suggests that (unless the signal T_u is negatively skewed) the mean radiation load on the substrate could be shed by an upper surface temperature that, by virtue of its oscillation, had a mean value lower than that (T_0) which would be required for a static balance (i.e. in the reference state).

2.4. Rigorous steady-state solution

A rigorous algebraic solution can be obtained if the device is in steady state, under forcing by a constant net radiation L^*, because in this case it is clear the temperature profile must be linear. Let $L_\downarrow = L_\uparrow + A = \sigma T_0^4 + A$ where T_0 is a 'background' temperature, so that the (steady) net radiation is $L_* = A$.

Because it simplifies the algebra, in this section we introduce the coordinate $\zeta = z + d/2$ and write the trial (steady state) solution as $T(z) = \alpha + \beta\zeta$, which trivially satisfies Eq. (5), since $\partial/\partial\zeta \equiv \partial/\partial z$. The two boundary conditions furnish two equations in α, β. Using Eq. (4) gives:

$$\beta = \frac{\epsilon\sigma}{k}(\alpha^4 - T_0^4), \tag{9}$$

which establishes that the base temperature ($\alpha \equiv T_b$) must differ from the background temperature if there is to be a steady-state linear gradient in the substrate (e.g. if $A > 0$ it is necessary that $T_b > T_0$, in order that conductive heat supply towards the base be dissipated radiatively by an excess of $\epsilon \sigma T_b^4$ over the absorbed fraction, $\epsilon \sigma T_0^4$, of $L_\uparrow$). Substituting this result into Eq. (3) and rearranging gives:

$$\left[\alpha + \frac{d}{k}\epsilon\sigma(\alpha^4 - T_0^4)\right]^4 + \alpha^4 = 2T_0^4 + A\sigma^{-1}. \tag{10}$$

If $A = 0$, a solution is $\alpha = T_0$, $\beta = 0$. By setting $A = 1$ W m^{-2} we can solve numerically to obtain the (inverse of the) calibration factor, i.e. the top-bottom temperature difference $\Delta T = T_u - T_b = \beta d$ corresponding to unit net radiation (we name this quantity "γ" [K (W m^{-2})$^{-1}$]). We shall see that this proves to be consistent with

the 'textbook' calibration factor γ^T defined by Eq. (24) in Section 2.5, and it provides a useful check on the numerical method we later use to obtain dynamic solutions (Section 3).

2.4.1. Uniqueness of solutions

Before proceeding to the textbook calibration and a more general, dynamic calibration, it is useful to prove that our idealized radiometer problem has a *unique* solution. The proof begins by positing that $T_1(z,t)$ and $T_2(z,t)$ are (arbitrary) solutions to Eqs. (3)–(6), and we introduce their difference, $\phi(z,t) = T_1 - T_2$. If it can be proven that ϕ vanishes for all time, it follows that (any) solution is unique.

The reader will at once see that ϕ, being a linear superposition of known solutions to the heat equation, satisfies the heat equation; and that its initial value is $\phi(z,0) = 0$. The boundary conditions controlling its subsequent evolution are

$$0 = -\epsilon\sigma(T_{1u}^4 - T_{2u}^4) - k\left(\frac{\partial\phi}{\partial z}\right)_u, \tag{11}$$

$$0 = -\epsilon\sigma(T_{1b}^4 - T_{2b}^4) + k\left(\frac{\partial\phi}{\partial z}\right)_b, \tag{12}$$

and may be re-written:

$$\left(\frac{\partial\phi}{\partial z}\right)_u = -\frac{\epsilon\sigma B_u(t)}{k}\phi_u, \tag{13}$$

$$\left(\frac{\partial\phi}{\partial z}\right)_b = +\frac{\epsilon\sigma B_b(t)}{k}\phi_b, \tag{14}$$

where

$$B_u(t) = [T_{1u}^2 + T_{2u}^2](T_{1u} + T_{2u}) \geq 0, \tag{15}$$

$$B_b(t) = [T_{1b}^2 + T_{2b}^2](T_{1b} + T_{2b}) \geq 0. \tag{16}$$

It is probably already clear (intuitively) that the difference $\phi = T_1 - T_2$ between (putatively) distinct general solutions not only is initially zero, but must remain so for all time. A completing (formal) argument that ϕ remains zero is readily given by consideration of the 'energy equation' (Zauderer, 1989) associated with the heat equation, viz.:

$$\phi\frac{\partial\phi}{\partial t} = \kappa\phi\frac{\partial^2\phi}{\partial z^2} \tag{17}$$

or

$$\frac{\partial\phi^2}{\partial t} = 2\kappa\left[\frac{\partial}{\partial z}\left(\phi\frac{\partial\phi}{\partial z}\right) - \left(\frac{\partial\phi}{\partial z}\right)^2\right]. \tag{18}$$

Integrating on $-d/2 \leq z \leq d/2$ one obtains the result that

$$\frac{\mathrm{d}}{\mathrm{d}t}\int_b^u \phi^2(z,t)\,\mathrm{d}z \leq 0 \tag{19}$$

and since the initial value of this integral vanishes, so do all subsequent values. Thus if once we can find a solution for the temperature profile in our radiometer, we can be sure it is the unique solution. The significance of this section is that a numerical solution, provided it entails negligible discretization error, can be accepted as a good approximation to the exact (but unknown) solution.

2.5. The textbook treatment

The well-known textbook analysis of the thermometric net radiometer (e.g. Fritschen, 1963; Fritschen and Gay, 1979, p. 96; Szeicz, 1975, p. 236), and indeed the very concept of the device,

apparently originated[2] with Albrecht (1933). Albrecht's treatment eliminates heat transfer within the substrate from further consideration, by invoking the restriction:

$$k\left(\frac{\partial T}{\partial z}\right)_u = k\left(\frac{\partial T}{\partial z}\right)_b = k\frac{T_u - T_b}{d}. \tag{20}$$

Here the conductive flux to/from the upper face is taken to be identical to the conductive flux from/to the lower face, and both are parameterized in terms of the finite difference $(T_u - T_b)$. One takes the difference between Eqs. (3) and (4):

$$0 = \epsilon(L_\downarrow - L_\uparrow) - \epsilon\sigma(T_u^4 - T_b^4) - 2k\left(\frac{T_u - T_b}{d}\right) \tag{21}$$

and with the aid of a linearization:

$$T_u^4 \approx T_b^4 + \left(\frac{dT^4}{dT}\right)_{T=T_b}(T_u - T_b) = T_b^4 + 4T_b^3(T_u - T_b) \tag{22}$$

one arrives at the textbook calibration:

$$\epsilon L^* = (T_u - T_b)\left[4\epsilon\sigma T_b^3 + \frac{2k}{d}\right] \tag{23}$$

or

$$\frac{T_u - T_b}{L^*} \equiv \gamma^T = \epsilon\left[4\epsilon\sigma T_b^3 + \frac{2k}{d}\right]^{-1} \tag{24}$$

(in the textbook derivation a term in the square bracket that arises from convective coupling would be included, then eliminated as a presumed consequence of the intervention of the 'domes'). Inserting plausible values shows the term in T_b^3 can be neglected in favour of $2k/d$. Thus the substrate conductivity emerges as the factor controlling the steady-state (static) calibration factor: the weaker the conductive coupling between the two faces, the greater the temperature difference that must prevail at steady state.

Now Eq. (20), in conjunction with Eqs. (3) and (4), gave us a system of three equations in three unknowns: $T_u, T_b, (\partial T/\partial z)_u$. The above 'textbook approximation' results from *subtracting* Eqs. (3) and (4). We may, instead, *add*. This eliminates the conductive heat flux term (but of course only subject to the validity of Eq. (20), and gives another equation complementing Eq. (23), viz.:

$$0 = \epsilon(L_\downarrow + L_\uparrow) - \epsilon\sigma(T_u^4 + T_b^4), \tag{25}$$

where the sum $L_\downarrow + L_\uparrow$ of the two longwave irradiances (both positive, by definition) is (of course) not the same quantity as the environmental net longwave radiation, $L^* \equiv (L_\downarrow - L_\uparrow)$. Eq. (25) is correct under the assumption it has invoked, namely a time-invariant and linear temperature gradient, in turn implying steady state: it simply says that, in that steady state, the conductive transport of heat within the substrate does not affect the overall energy balance and the total rate of longwave emission from the device must equal its total rate of absorption of incoming longwave radiation. This is obvious, and consistent with the result obtained by integrating Eq. (5) across the device, viz.:

$$c\frac{\partial}{\partial t}\int_{-d/2}^{d/2} T(z,t)\,dz = cd\frac{\partial\overline{T}}{\partial t} = \left(k\frac{\partial T}{\partial z}\right)_u - \left(k\frac{\partial T}{\partial z}\right)_b, \tag{26}$$

where $\overline{T}$ is the mean temperature of the radiometer slab (if the temperature profile in the substrate were linear, then $\overline{T} = (T_u + T_b)/2$). Upon eliminating the conduction terms by application of the boundary conditions (Eqs. (3) and (4)) this yields:

$$cd\frac{\partial\overline{T}}{\partial t} = \epsilon(L_\downarrow + L_\uparrow) - \epsilon\sigma(T_u^4 + T_b^4) \tag{27}$$

and in steady state we recover Eq. (25).

An interesting result emerges if one weights each term in the heat equation (Eq. (5)) by position, before integrating across the slab. The property:

$$s(t) = \int_{-d/2}^{d/2} z\,T(z,t)\,dz \tag{28}$$

should be proportional to the signal[3] ΔT, and obeys:

$$c\frac{\partial s}{\partial t} = \int_{-d/2}^{d/2} z\frac{\partial^2 T}{\partial z^2}\,dz, \tag{29}$$

which upon integration by parts gives the result:

$$c\frac{\partial s}{\partial t} = \epsilon(L_\downarrow - L_\uparrow) - \epsilon\sigma(T_u^4 - T_b^4) - 2k\left(\frac{T_u - T_b}{d}\right). \tag{30}$$

This generalizes Eq. (21) to non-steady conditions.

3. Numerical analysis

We would like to know (in the most general terms) the response of the output $\Delta T(t)$ to the forcing $L^*(t) = L_\downarrow(t) - L_\uparrow(t)$. The device is non-linear, it will certainly exhibit inertia, and it may well exhibit hysteresis (implying the relationship between ΔT and L^* is not single-valued; hysteresis is an observed property of some radiometers, e.g. Halldin and Lindroth, 1992). Standard approaches of 'linear systems theory' would be to try to derive the step response, and the sinusoidal response, both of which are implied by the transfer function (ratio of the Laplace transform of the output to Laplace transform of the input). Here we shall calculate (numerically) the full response of the radiometer out to a time $t \gg \tau$ (the device time constant), when initialized in an isothermal state T_0, and driven by irradiances:

$$\begin{aligned}L_\downarrow(t) &= \sigma T_0^4 + A\sin(2\pi ft), \\ L_\uparrow &= \sigma T_0^4\end{aligned} \tag{31}$$

such that $L^*(t) = A\sin(2\pi ft)$.

In this section it is to be understood that T represents the *deviation* of the temperature from the background temperature T_0, this last in Kelvin units. The differential equation and boundary conditions have been transformed into a closed set of algebraic relations between the temperature deviations T_J at a set of gridpoints located at

$$z(J) = J\frac{d}{2N}, \quad J = -N\ldots N \tag{32}$$

(grid interval $\Delta z = d/(2N)$), where for all simulations to be shown, $N = 499$. At each internal gridpoint ($|J| < N$) the heat equation was discretized using the Crank–Nicolson scheme:

$$\begin{aligned}\frac{T_J^n - T_J^{n-1}}{\Delta t} &= \frac{\kappa}{2\Delta z^2}[T_{J+1}^n + T_{J-1}^n - 2T_J^n] \\ &\quad + \frac{\kappa}{2\Delta z^2}[T_{J+1}^{n-1} + T_{J-1}^{n-1} - 2T_J^{n-1}],\end{aligned} \tag{33}$$

which is second-order accurate in $\Delta t, \Delta z$.

---

[2] Suomi et al. (1954) stated that Albrecht (1933) had "shown that the net radiation can be obtained very nearly by exposing a blackened plate parallel to the earth's surface and measuring the temperature difference existing through it." A colleague's reading of the original Albrecht (1933) supports our inference that Albrecht originated the principle of the familiar thermometric net radiometer. It is perhaps appropriate to reiterate here a statement of Smith et al. (1997), based on their careful examination of the response of numerous net radiometers: "We find a fundamental deficiency in the two-sided thermopile design used in most net pyrradiometers under non-equilibrium conditions."

---

[3] Certainly it is in steady state, for then the temperature profile is linear.

Table 1

Simulations of response of radiometer (with properties defined in Section 3.2) to sinusoidal forcing of the downward longwave irradiance with amplitude A and frequency f. Background temperature $T_0 = 293.16$ K. The rightmost column gives the equivalent error in measured net radiation induced by the oscillating net radiative forcing, obtained by combining the computed steady-state calibration factor with the radiometer's computed mean signal $\overline{\Delta T} = \overline{T}_u - \overline{T}_b$ defined over exactly one cycle $1/f$, beginning 10τ after initialization in the isothermal state. (Simulated values for the temperature of the lower plane and the top–bottom temperature difference, under forcing by a steady difference of 1 W m^{-2}, were $T_b = \alpha^{\mathrm{Num}} = 293.2412$ K, $\Delta T = \gamma^{\mathrm{Num}} = 0.00624295$ K.)

$f\,[\mathrm{s}^{-1}]$	$f\tau$	λ (mm)	A (W m^{-2})	$A/(4\sigma T_0^3)$ (K)	$\overline{\Delta T}$ (K)	$A_T(d/2)$ (K)	$\sigma[\overline{T_t^4} - \overline{T}_t^4]$ (W m^{-2})	$\overline{\Delta T}(4\sigma T_0^3)/A$	$\overline{\Delta T}/\gamma^{\mathrm{Num}}$ (W m^{-2})
0.005	0.175	2.862	10	1.75	$+2.6 \times 10^{-5}$	8.0×10^{-2}	9.0×10^{-5}	$+1.47 \times 10^{-5}$	$+4.1 \times 10^{-3}$
0.05	1.749	0.905	10	1.75	$+7.5 \times 10^{-7}$	2.7×10^{-2}	1.1×10^{-5}	$+4.3 \times 10^{-7}$	$+1.2 \times 10^{-4}$
0.5	17.49	0.286	10	1.75	-1.7×10^{-7}	9.0×10^{-3}	1.1×10^{-6}	-9.8×10^{-8}	-2.7×10^{-5}
0.05	1.749	0.905	50	8.75	$+1.8 \times 10^{-6}$	1.4×10^{-1}	2.8×10^{-4}	$+2.0 \times 10^{-6}$	$+2.8 \times 10^{-4}$
0.05	1.749	0.905	200	35.0	-1.4×10^{-5}	5.5×10^{-1}	4.4×10^{-3}	$+4.3 \times 10^{-7}$	-2.2×10^{-3}

3.1. Tridiagonal system

If the temperature gradients on upper and lower faces are discretized in the crudest and most obvious manner:

$$\left(\frac{\partial T}{\partial z}\right)_u^n = \frac{T_N^n - T_{N-1}^n}{\Delta z},$$
$$\left(\frac{\partial T}{\partial z}\right)_b^n = \frac{T_{-N+1}^n - T_{-N}^n}{\Delta z} \quad (34)$$

the complete closed system of equations constitutes a tridiagonal matrix inversion problem, with the penalty that the above 'computational molecules' are only first order accurate in Δz (in principle, this inelegant choice may be compensated by refining Δz to keep discretization error at an acceptable level).

Of course it is necessary to linearize the boundary conditions, which has been done as follows (we show only the upper surface). First, let $^{(m)}T_J^n$ represent the mth iteration towards an eventual converged estimate T_J^n of the temperature deviation at the 'new' time (n). Then taking the first term in a Taylor expansion, we may write (temporarily suppressing the indices n,J):

$$[T_0 + {}^{(m)}T]^4 \approx [T_0 + {}^{(m-1)}T]^4 + 4[T_0 + {}^{(m-1)}T]^3[{}^{(m)}T - {}^{(m-1)}T]. \quad (35)$$

In this spirit, the upper boundary condition is discretized:

$$\left[\frac{4\epsilon\sigma}{\rho_s c_s}[T_0 + {}^{(m-1)}T_N^n]^3 + \frac{\kappa}{\Delta z}\right]{}^{(m)}T_N^n = \frac{\kappa}{\Delta z}{}^{(m)}T_{N-1}^n$$
$$+ \frac{\epsilon}{\rho_s c_s}L_\downarrow(t)$$
$$+ \frac{4\epsilon\sigma}{\rho_s c_s}[T_0 + {}^{(m-1)}T_N^n]^3{}^{(m-1)}T_N^n$$
$$- \frac{\epsilon\sigma}{\rho_s c_s}[T_0 + {}^{(m-1)}T_N^n]^4$$

$$(36)$$

with a similar equation for the lower face (it may be helpful to write $T_* \equiv {}^{(m-1)}T_N^n$ as the known, latest provisional estimate). Having introduced this more complex terminology, we rewrite the Crank–Nicolson algorithm for the internal gridpoints:

$$\frac{{}^{(m)}T_J^n - T_J^{n-1}}{\Delta t} = \frac{\kappa}{2\Delta z^2}[{}^{(m)}T_{J+1}^n + {}^{(m)}T_{J-1}^n - 2{}^{(m)}T_J^n]$$
$$+ \frac{\kappa}{2\Delta z^2}[T_{J+1}^{n-1} + T_{J-1}^{n-1} - 2T_J^{n-1}], \quad (37)$$

where the *lack* of the supplementary iteration counter (m) at time level ($n - 1$) emphasizes known values at the 'prior time' that do *not* evolve during the iteration.

For the solutions to follow, the timestep $\Delta t = (1/f)/M$, where $M = 10^4$ (note: the Crank–Nicolson scheme is unconditionally stable, and the choice of such a small timestep was made in order that we should evaluate the response of the device over an exact

number of cycles in the forcing, so as not to spuriously infer the existence of an offset that might be nothing more than a consequence of inexactness in the numerical integration). The inner loop was iterated (to a limit $m \le 50$) so long as $\max_{(\mathrm{all}\,J)}\{|{}^{(m)}T_J - {}^{(m-1)}T_J|\} > 10^{-18}$ K. The reader will probably expect that the response of the temperature in the substrate to sinusoidal forcing would be sinusoidal, but as we do not have a linear system it is worthwhile to be explicit: but for a decaying initial phase (discussed later), the computed response was indeed sinusoidal[4].

3.2. Specification of the case study

The following solutions pertain for the case:
$d = 0.003$ m,
$\rho_s = 1060$ kg m^{-3},
$c_s = 1613$ J kg^{-1}K^{-1},
$k = 0.22$ W K^{-1} m^{-1},
$\epsilon = 0.95$,
$T_0 = 20\,^{\circ}$C.

These substrate properties correspond to those of a generic epoxy (e.g. Sundqvist et al., 1977; Gustafsson et al., 1979); and they imply $\kappa = 1.29 \times 10^{-7}$ m^{2}s^{-1}, and (with $\alpha = 0.5$ in Eq. (2)) $\tau = 35.0$ s.

3.3. Steady state—(analytical)

The steady-state base temperature $T_b = \alpha$ for the case of a steady net radiation $L^* = 1$ W m^{-2} was determined, by finding the zero crossing(s) of Eq. (10) using a simple search covering range $T_0 \pm 20$ K, with resolution $\Delta\alpha = 10^{-6}$ K. A single zero was identified on this range, at $\alpha = 293.24$ K, i.e. $T_b - T_0 = 0.08$ K at steady state with $L^* = 1$W m^{-2}. The steady-state sensitivities (calibration factors) are

$$\gamma^{\mathrm{T}} = 0.0062461\ \mathrm{K}(\mathrm{W\ m}^{-2})^{-1},$$
$$\gamma = 0.0062460\ \mathrm{K}(\mathrm{W\ m}^{-2})^{-1}$$

where γ^{T} is the linearized 'textbook' value, and γ was obtained from Eq. (9). That these estimates compare favourably with the value ($\gamma^{\mathrm{Num}} = 0.00624295$) obtained by numerical solution is evidence for the reasonable accuracy of the latter.

3.4. Computed sinusoidal response

For the results to be reported (Table 1), the longwave radiation beams were specified by Eq. (31). Table 1 documents the computed behaviour of the radiometer, for frequencies $f = (0.005, 0.05, 0.5)$ Hz, and for several forcing amplitudes. The amplitude ("A_u" = $A_T(d/2)$) of the cycle in the temperature T_u of the upper surface is rather small, such that the distinction between

---

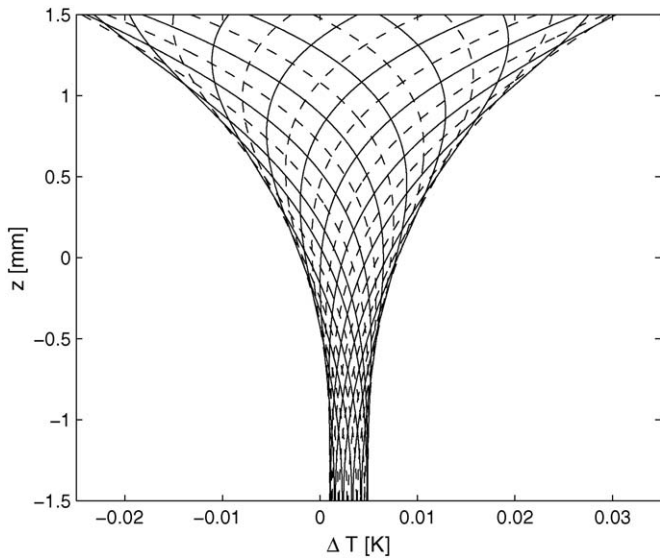[4] Contrary to what was anticipated in Section 2.2.

Fig. 2. Numerically simulated profiles of temperature deviation away from the background temperature T_0, during one cycle of forcing ($f = 0.05$ Hz, $A = 10$ W m^{-2}) and plotted at intervals $0.04/f$. The amplitude of the temperature wave at the upper surface, determined from the ensemble of profiles at intervals $\Delta t = 10^{-4}(1/f)$, was $A_u \equiv A_T(d/2) = 0.0275$ K.

$\sigma \overline{T_u^4}$ and $\sigma \overline{T_u}^4$ (W m^{-2}) is practically insignificant (and in accordance, incidentally, with Eq. (8)). Consequently, there is no appreciable bias: the mean value $\overline{\Delta T} \equiv \overline{T_u} - \overline{T_b}$ is negligible. In hindsight, had we considered the plausible magnitude of the waves in surface temperatures T_u, T_b likely to be induced by plausible field fluctuations in $L_\downarrow$, $L_\uparrow$, we should have reached this conclusion by a much quicker, albeit heuristic, argument.

Fig. 2 shows the behaviour of the temperature wave over a single forcing cycle (for the case $f = 0.05$ Hz), commencing at $t/\tau = 10$ (where $\tau = 35$ s is the device time constant). The amplitude $A_T(z)$ of the driven oscillation in the radiometer's temperature is expected to decay on damping depth:
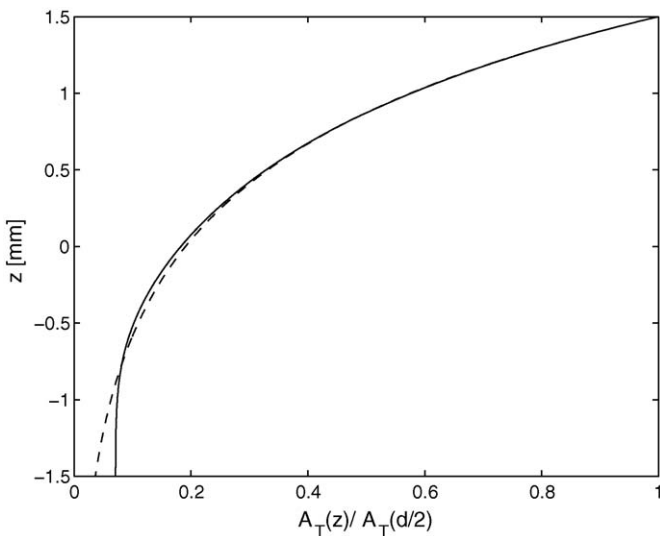
$$\lambda = \sqrt{\kappa/(\pi f)}, \tag{38}$$

Fig. 3. Attenuation with depth of the normalized amplitude $A_T(z)/A_T(d/2)$ of the temperature deviation from background temperature T_0, during one cycle of forcing ($f = 0.05$ Hz, $A = 10$ W m^{-2}). The dashed line gives the theoretical attenuation curve, viz. $\exp[-(d/2 - z)/\lambda]$, where for this case $\lambda = 0.905$ mm.
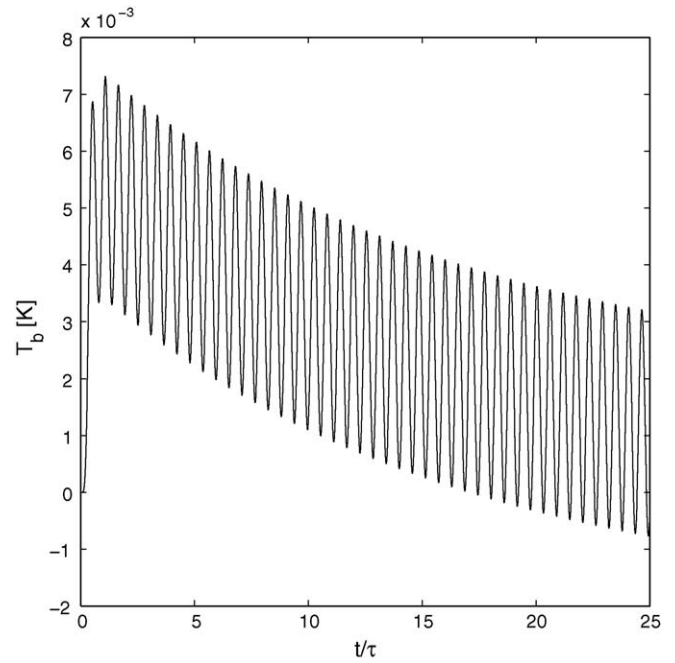

Fig. 4. Time variation of the temperature T_b at the base of the radiometer, with forcing frequency $f = 0.05$ Hz and amplitude $A = 10$ W m^{-2}. (The amplitude of the oscillation may be perceived as growing with t/τ, however this is an optical illusion.)

and Fig. 3 shows that broadly speaking the computed attenuation matches expectation, however with a systematic departure far from the surface (normalization forces the match at the upper surface $z = d/2$).

Returning to Fig. 2, we note that the damped oscillation in T_b, seen in snapshots across a forcing single cycle, is *not centred* on zero (that is, not centred on $T_b = T_0$). Fig. 4, a plot of $T_b(t)$, shows that the centre point of the oscillation steps promptly away from T_0 when excitation commences at $t = 0$, then relaxes on a rather a long timescale, such that by about $t/\tau \sim 100$ the oscillation is centred on T_0 (here again, τ is the intrinsic time constant from Eq. (2), evaluated with $\alpha = 1/2$). We did not anticipate this long transient, and are unsure whether it is a numerical artifact, or a real facet of this non-linear device.

4. Conclusion

Our results show that, if there *is* a calibration bias in the sense defined earlier, then it is so small (for plausible amplitudes of the variation in radiative forcing) as to be of no practical importance. Of course having investigated the question *numerically*, owing to the existence of discretization and machine roundoff error we cannot (and do not) say such a bias is absolutely *non-existent*: to the contrary, we believe a small bias *does* exist – based on the reasoning of Section 2.3.

Real net radiometers are much more complex than the idealized device studied here, e.g. by virtue of convective heat exchange, and radiative interaction with the dome used to eliminate it. Others (e.g. Albrecht et al., 1974; Albrecht and Cox, 1977) have long ago derived and tested calibration formulae accounting for this aspect. Nonetheless (Smith et al., 1997), reporting their detailed laboratory and field investigation of a representative range of real net radiometers, noted that most radiometers had a "longer ramp-down response than ramp-up response," a phenomenon which eludes (i.e. whose origin lies outside) the simplistic model adopted here; by driving the "numerical radiometer" with an upward or downward step (of magnitude up to 100 W m^{-2}) in (alternatively) $L_\downarrow$ or $L_\uparrow$, we found (as one would suspect from the equations) that

the response was completely symmetrical. Smith et al. concluded "A theoretical analysis of net pyrradiometer design, in conjunction with the conductivity tests, suggest that this type of radiometer is always susceptible to uncertainty errors of 5–10% when used in actual field conditions because the thermal steady-state/zero flow assumptions under which the instruments are calibrated are not valid for a realistic measuring environment" (see also Halldin et al., 1999). Our having here proven the insignificance of a particular bias that originates from non-linearity of the boundary conditions does not assuage the concern that these conclusions of Smith et al. (and others since) have prompted.

Acknowledgments

References

Albrecht, B., Cox, S.K., 1977. Procedures for improving pyrgeometer performance. J. Appl. Meteorol. 16, 188–197.

Albrecht, B., Peollet, M., Cox, S.K., 1974. Pyrgeometer measurements from aircraft. Rev. Sci. Instrum. 45, 33–38.

Albrecht, F., 1933. Ein Strahlungsbilanzmesser Zur Messung Des Strablungshaush-altes Von Ober achen. Meteorol. Zeitschrift 50, 62–65.

Brotzge, J.A., Duchon, C.E., 2000. A field comparison among a domeless net radio-meter, two four-component net radiometers, and a domed net radiometer. J. Atmos. Ocean. Technol. 17, 1569–1582.

Cobos, D.R., Baker, J.M., 2003. Evaluation and modification of a domeless net radiometer. Agron. J. 95, 177–183.

Fritschen, L.J., 1963. Construction and evaluation of a miniature net radiometer. J. Appl. Meteorol. 2, 165–172.

Fritschen, L.J., 1965. Miniature net radiometer improvements. J. Appl. Meteorol. 4, 528–532.

Fritschen, L.J., Gay, L.W., 1979. Environmental Instrumentation. Springer-Verlag.

Funk, J.P., 1960. Transient response of net radiometers. Theor. Appl. Climatol. 10, 228–231.

Gustafsson, S.E., Karawackif, E., Nazim Khan, M., 1979. Transient hot-strip method for simultaneously measuring thermal conductivity and thermal diffusivity of solids and fluids. J. Phys. D. 12, 1411–1421.

Halldin, S., Lindroth, A., 1992. Errors in net radiometry: comparison and evaluation of six radiometer designs. J. Atmos. Ocean. Technol. 9, 762–783.

Halldin, S., Bergstrom, H., Gustafsson, D., Dahlgrend, L., Hjelma, P., Lundina, L.-C., Mellan-der, P.-E., Nord, T., Jansson, P.-E., Seibert, J., Stahli, M., Szilagyi Kishne, A., Smedman, A.-S., 1999. Continuous long-term measurements of soil–plant–atmosphere variables at an agricultural site. Agric. For. Meteorol. 98–99, 75–102.

Huang, J., Lee, X., Patton, E.G., 2008. A modelling study of flux imbalance and the influence of entrainment in the convective boundary layer. Boundary-Layer Meteorol. 127, 273–292.

Kohsiek, W., et al., 2007. The energy balance experiment EBEX. Part III: Behaviour and quality of the radiation measurements. Boundary-Layer Meteorol. 123, 55–75.

Mauder, M., Oncley, S.P., Vogt, R., Weidinger, T., Ribeiro, L., Bernhofer, C., Foken, T., Kohsiek, W., de Bruin, H.A.R., Liu, H., 2007. The energy balance experiment EBEX-2000. Part II: Intercomparison of eddy-covariance sensors and post-field data processing methods. Boundary-Layer Meteorol. 123, 29–54.

Philipona, R., Fröhlich, C., Betz, Ch., 1995. Characterization of pyrgeometers and the accuracy of atmospheric long-wave radiation measurements. Appl. Opt. 34, 1598–1605.

Smith, E.A., Hodges, G.B., Bacrania, M., Cooper, H.J., Owens, M.A., Chappell, R., Kincannon, W., 1997. Final Report [NASA Grant NAG5-2447] BOREAS Net Radiometer Engineering Study. Tech. rept. NASA.

Sundqvist, B., Sandberg, O., Bäckström, G., 1977. The thermal properties of an epoxy resin at high pressure and temperature. J. Phys. D. 10, 1397–1403.

Suomi, V.E., Franssila, M., Islitzer, N.F., 1954. An improved net-radiation instrument. J. Meteorol. 11, 276–282.

Szeicz, G., 1975. Instruments and their exposure. In: Monteith, J.L. (Ed.), Vegetation and the Atmosphere, vol. 1: Principles. Academic Press, (Chapter 7), pp. 229–273.

Zauderer, E., 1989. Partial Differential Equations of Applied Mathematics, 2nd edn. J. Wiley & Sons.